

# Dielectrophoretic Technique for Measurement of Chemical and Biological Interactions

Sang Hyun Baek,<sup>†</sup> Woo-Jin Chang,<sup>‡,§</sup> Ju-Yeoul Baek,<sup>†</sup> Dae Sung Yoon,<sup>†</sup> Rashid Bashir,<sup>\*,†</sup> and Sang Woo Lee<sup>\*,†</sup>

Department of Biomedical Engineering, Yonsei University, Wonju 220-710, Korea, Department of Electrical and Computer Engineering and Bioengineering, Micro and Nanotechnology Laboratory, University of Illinois at Urbana-Champaign, Champaign, IL 61820, and ERC for Advanced Bioseparation Technology, Inha University, Incheon 402-751, Korea

We present a novel dielectrophoretic technique that can be used to characterize molecular interactions inside a microfluidic device. Our approach allows functionalized beads which are initially at rest on a functionalized surface to be pulled away from the surface by the dielectrophoretic force acting on the beads. As a result, the interaction between the molecules on the surface and the beads can be quantitatively examined. We report detailed experimental results and validate the results with a model to show that the technique can be used to measure forces of interaction between molecules under various experimental conditions.

Examination of molecular interactions and forces is critical to the functional understanding of all chemical and biological systems. The prominent techniques for the direct measurement of these interactions at the single molecule level are atomic force microscopy (AFM),<sup>1,2</sup> optical tweezers,<sup>3,4</sup> and magnetic tweezers.<sup>5,6</sup> In the case of AFM, a sharp tip functionalized with molecules is brought close to a surface coated with complementary molecules. The forces can be characterized when the interaction is broken by the retraction of the tip from the surface. Optical and magnetic tweezers, on the other hand, can manipulate a functionalized particle to study the interactions between the particle and the surface with beams of light exerting photon energy on the particle in one case and magnetic forces on a paramagnetic particle in the other case. Through the observation of the movement of the particle, the intermolecular forces between the bead and the surface can be characterized. While the AFM and the optical tweezers are very powerful and have been utilized for various applications, they are serial in nature and provide the binding information on a single event. Hence, many measurements need to be performed serially to get statistics and distributions. The

AFM requires the probe tip to be brought close to the surface and simultaneous imaging is not easily possible, and optical tweezers require a laser beam to be focused on a particle for the manipulation of the bead, both one event at a time. The magnetic tweezers can be parallel; however, the approach is less attractive since a repulsive force needed for the measurement procedures is complicated by the lack of a single magnetic pole and by the fact that the repulsive force scales as fourth power of the dimension of integrated microcoils. In contrast, the proposed technique is parallel (many events can be interrogated at the same time), cheap, and easy to implement, the force scales as the second power of the dimension of a simple interdigitated (IDT) electrode array, and the technique can also be used within a microfluidic device.<sup>7</sup> In the present work, we report on the detailed experimental examination of this dielectrophoretic technique for examining the forces between a functionalized particle and a functionalized surface under different chemical conditions to demonstrate the utility of this approach. We also develop a model to analyze the intermolecular interactions based on the experimental results using various conditions and compare our results to prior work reported by others.

## EXPERIMENTAL SECTION

**Micro-Chip Fabrication.** Photolithography techniques were used to define an interdigitated (IDT) electrode array where each metal line was 40  $\mu\text{m}$  wide and 10  $\mu\text{m}$  apart on an oxidized silicon wafer for subsequent lift-off process. A 0.2  $\mu\text{m}$  thick chromium layer was deposited using a thermal evaporator and subsequently patterned using a lift-off process. The metal electrodes were covered by a 0.8  $\mu\text{m}$  thick plasma-enhanced chemical vapor deposited (PECVD) silicon dioxide from a TEOS (tetraethylorthosilicate) source.

**Preparation of Functionalized Silicon Oxide Surfaces on the Chip.** Three different functionalized oxide surfaces were prepared using 3-aminopropyltriethoxysilane (APTES, Sigma-Aldrich, A3648), succinic anhydride (Aldrich, 239690), or L-lysine (Sigma, L5501). (1) For an amino-terminated APTES self-assembly monolayer (SAM), the modified Stöber method<sup>8</sup> was used. First, the fabricated chip having the IDT structure was transferred into a solution consisting of  $\text{H}_2\text{SO}_4$ – $\text{H}_2\text{O}_2$  (1:1), resulting in a clean hydroxyl-functionalized oxide surface. After rinsing the sub-

\* To whom correspondence should be addressed. E-mail: yusuklee@yonsei.ac.kr (S.W.L.); rbashir@illinois.edu (R.B.).

<sup>†</sup> Yonsei University.

<sup>‡</sup> University of Illinois at Urbana-Champaign.

<sup>§</sup> Inha University.

(1) Tos, R.; et al. *Proc. Natl. Acad. Sci. U.S.A.* **1998**, *95*, 7402–7405.  
(2) Wielert-Badt, S.; et al. *Biophys. J.* **2002**, *82*, 2767–2774.  
(3) Liang, M. N.; et al. *Proc. Natl. Acad. Sci. U.S.A.* **2000**, *97*, 13092–13096.  
(4) Bjornham, O.; et al. *J. Biomed. Opt.* **2005**, *10* (1–9), 044024.  
(5) Gosse, C.; Croquette, V. *Biophys. J.* **2002**, *82*, 3314–3329.  
(6) Assi, F.; Jenks, R.; Yang, J.; Love, C.; Prentiss, M. *J. Appl. Phys.* **2002**, *92*, 5584–5586.

(7) Lee, S. W.; Chang, W.-J.; Bashir, R.; Koo, Y.-M. *Biotechnol. Bioprocess. Eng.* **2007**, *12*, 185–199.

(8) An, Y.; Chen, M.; Xue, Q.; Liu, W. *J. Colloid Interface Sci.* **2007**, *311*, 507–513.

strate with DI water, it was immersed into the ethanol dissolving 10 mM APTES to create the amino-terminated SAM on the oxide surface. The substrate was baked inside an oven at 120 °C for 1 h after removing the APTES residue through rinsing ethanol and DI water. (2) The succinic anhydride SAM with one carboxyl-terminated molecule in the tail group on the oxide surface was created using the substrate already having an amino-terminated APTES SAM. After 0.1 M succinic anhydride was dissolved in DMF (*N,N*-dimethylformamide, Sigma-Aldrich, D158550) solution, the amino-functionalized substrate was placed into the solution for 24 h. As a result, the carboxyl-terminated SAM layer was generated on the oxide surface. For the removal of the succinic anhydride residue, the substrate was cleaned with DMF and DI water. (3) In order to form the L-lysine self-assembled monolayer consisting of two amino-terminated molecules in the tail group, the oxide surface in the fabricated chip was cleaned with acetone and methanol solution, rinsed in a solution of 20 mL of H<sub>2</sub>O, 30 mL of ethanol, 5 g of NaOH, and then rinsed in DI water, sequentially. A plasma etcher was used to clean the chip for 20 min after feeding oxygen gas into the etcher. Subsequently, L-lysine solution at 0.1 mg/mL was introduced onto the chip and incubated for 1 h at 37 °C. To remove the L-lysine residue, the chip was intensively rinsed with DI water.

**Experimental Procedures.** After forming a PDMS (polydimethylsiloxane) reservoir on each functionalized surface, two different experiments were performed. For the investigation of the interaction between carboxyl molecules or carboxyl-amino molecules on the beads and the surface, the solution containing the 15 μm diameter beads functionalized with a carboxyl group (Spherotech Inc. CPX-150-10 at a concentration of 1.34 × 10<sup>6</sup> beads/mL) was introduced onto a succinic anhydride functionalized oxide surface or L-lysine functionalized oxide surface, respectively. The other experiment was used for the solution containing the 10 μm diameter beads functionalized with an amino group (Spherotech Inc., AP-100-10, at a concentration of 1.34 × 10<sup>6</sup> beads/mL) in combination with the APTES functionalized surface or the L-lysine functionalized surface to study the interaction between amino molecules on the bead and the surface. The pH of both solutions was controlled by adding 1–50 μL of NaOH solution or HCl solution into the 20 mL solution containing the beads. The reservoir was covered by a glass slide, and the beads were allowed to settle and interact with the surface for 10 min. The movement of beads was observed under a microscope and recorded through a CCD camera while a sinusoidal signal at 10 MHz with different peak voltages was applied to the electrode array using micromanipulator probes.

## RESULTS AND DISCUSSION

**Measurement of Unbinding Voltages to Break Intermolecular Interaction between the Molecules on the Beads and the Surface.** When applying AC voltage with 10 MHz into the chip, the beads move away from the regions of the highest field gradient (i.e., negative dielectrophoresis force) since the Clausius-Mossotti factor<sup>9</sup> is negative:

$$\text{Re}[K(\omega)] = \text{Re} \left[ \frac{\bar{\epsilon}_p - \bar{\epsilon}_m}{\bar{\epsilon}_p + 2\bar{\epsilon}_m} \right] \quad (1)$$

where  $\bar{\epsilon}_p$  and  $\bar{\epsilon}_m$  are complex permittivity of the microbeads and the medium, respectively (bulk conductivity and permittivity of polystyrene bead = 2.4 × 10<sup>-4</sup> S/m and 2.6ε<sub>0</sub> and conductivity and permittivity of DI water = 1.5 × 10<sup>-4</sup> S/m and 78ε<sub>0</sub>). As schematically shown in Figure 1a, negative dielectrophoretic forces would move the beads at the edges of the IDT electrodes to the middle, and the beads at the middle of the IDT electrodes would be levitated above the electrodes breaking away any interactions between the beads and the oxide surface. Figure 1b–d shows optical images of the IDT structures depicting that the beads which were not located at the middle of IDT structures were first moved to the middle of IDT structures, noting that the negative DEP force used to pull the beads away from the surface is only in the vertical direction at the middle of IDT electrodes.<sup>10</sup> After increasing the voltage further, the beads were eventually removed from the surface, as shown by the defocusing of the beads in the optical images in Figure 1e. The images were taken sequentially as the increment of a voltage. On the basis of the observation of the behavior of the beads, the voltage at which more than 90% of the beads were detached simultaneously from the surface was defined as the “unbinding voltage”, i.e., the voltage which represents the strength of the interaction between the bead and surface. Figure 2 shows the plot of the percentage of beads removed from the surface as a function of the applied voltage at a few representative conditions depicting the extraction of the unbinding voltage. This experimental approach was used to measure the unbinding voltage at various pH conditions, as shown in Figure 3, for the following specific molecules: (i) carboxyl-coated beads and succinic anhydride functionalized surfaces presenting a carboxyl group, (ii) amino-coated beads and APTES functionalized surfaces, (iii) amino-coated bead and L-lysine functionalized surfaces, and (iv) carboxyl-coated beads and L-lysine functionalized surfaces. Moreover, in order to investigate a diffuse double layer affecting the molecular interactions, the unbinding voltages between the carboxyl-coated beads and the L-lysine surfaces at pH 7, the amino-coated beads and the APTES functionalized surface at pH 12, and the carboxyl-coated beads and the succinic anhydride functionalized surface at pH 4 were explored by adding sodium chloride to the medium. The variation of the resulting voltages versus the salt concentration is shown in Table 1. The observed unbinding voltage between the carboxyl-coated beads and the amino-groups in the L-lysine functionalized surface at pH 7 is attributed to ionic binding because the theoretical acid dissociation constants (pK<sub>a</sub>) of carboxyl group and amino group of L-lysine are below 5<sup>11</sup> and above 9,<sup>12</sup> respectively. At pH 12, the unbinding voltage between the neutralized amino-terminated beads and the neutralized amino group in APTES functionalized surface, where the pK<sub>a</sub> of amino group of APTES is 11,<sup>13</sup> can be attributed to a hydrophobic interaction. The

(10) Lee, S. W.; Li, H.; Bashir, R. *Appl. Phys. Lett.* **2007**, *90*, 223902.

(11) Fu, S.; Li, D.; Lucy, C. A. *Analyst* **1998**, *123*, 1487–1492.

(12) [http://www.chemie.fu-berlin.de/chemistry/bio/aminoacid/lysin\\_en.html](http://www.chemie.fu-berlin.de/chemistry/bio/aminoacid/lysin_en.html).

(13) Guillot, M.; Richard-Plouet, M.; Vilminot, S. *J. Mater. Chem.* **2002**, *12*, 851–857.

(9) Pohl, H. A. *Dielectrophoresis*; Cambridge University Press: Cambridge, U.K., 1978.

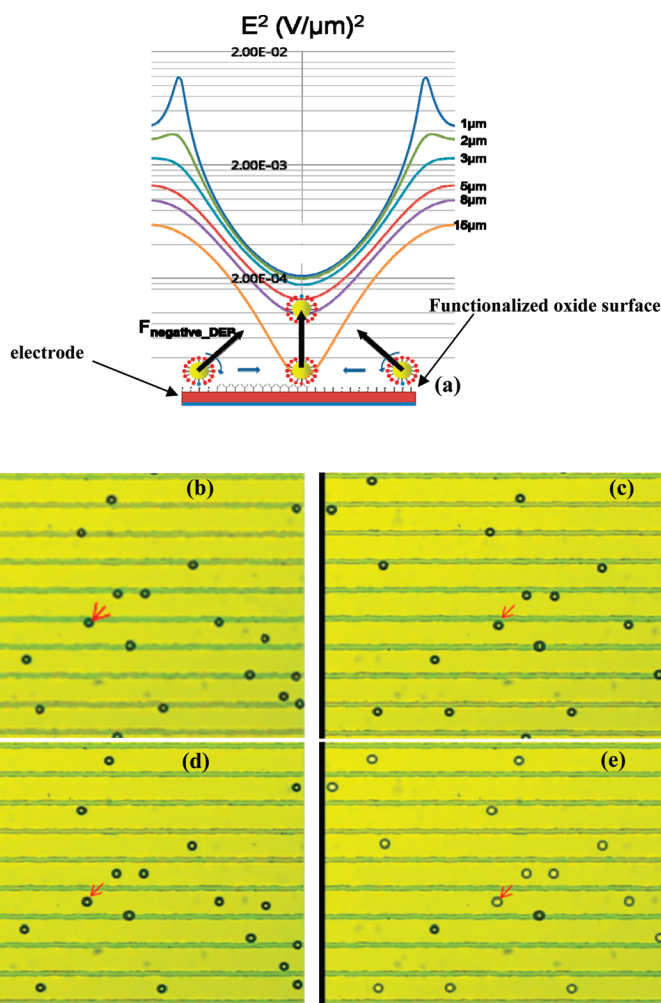


**Figure 1.** (a) Square of electric field of the IDT structure with  $40\ \mu\text{m}$  width and  $10\ \mu\text{m}$  space and a schematic diagram depicting the lateral and vertical movement under a negative DEP force. (b–d) Optical image of the lateral movement toward the center of electrode. (e) Optical image of the beads removed completely from the oxide surface and levitated above the center of electrode.

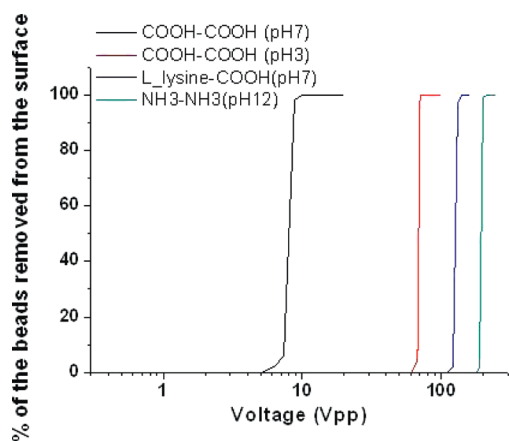


**Figure 2.** Percentage of beads repelled away from the oxide surface as the function of voltage for certain chemical molecules and pH conditions to demonstrate the extraction of the “unbinding voltage”.

hydrogen bonding can be the cause of the unbinding voltage between the carboxyl-coated beads and the carboxyl-group in the succinic anhydride functionalized surface at pH 4 since the  $pK_a$  of the carboxyl-group in the succinic anhydride is 4.2.<sup>14</sup> On the basis of the results in Table 1, the diffuse double layer generated by the sodium chloride only affected the

unbinding voltage due to its dependence on the ionic binding between the carboxyl-coated beads and the amino group in L-lysine functionalized surface. As the concentration of sodium chloride is increased, the charge screening effect<sup>15</sup> due to the diffuse double layer generated by the sodium and chloride ions in the medium is increased, resulting in the gradual decrease of the unbinding voltage, as shown in Table 1 (footnote a). The variations of the unbinding voltage shown in Table 1 (footnotes b and c) are not related to the electrostatic interaction generated by the diffuse double layer since the decrease of the unbinding voltage is different from that of the unbinding voltage by the charge screening effect represented between the carboxyl-coated beads and the amino group in the L-lysine functionalized surface at pH 7. It might be caused by the  $pK_a$  shift of the amino and carboxyl groups due to an increase in the salt concentration, as reported by previous papers.<sup>16,17</sup>

- (14) Biswas, A.; Shogren, R. L.; Kim, S.; Willett, J. L. *Carbohydr. Polym.* **2006**, *64*, 484–487.
- (15) Zhang, J.; Yoon, R.; Mao, M.; Ducker, W. A. *Langmuir* **2005**, *21*, 5831–5841.
- (16) Lee, K. K.; Fitch, C. A.; Lecomte, J. T. J.; Garcia-Moreno, E. B. *Biochemistry* **2002**, *41*, 5656–5667.
- (17) [http://en.wikipedia.org/wiki/Acid\\_dissociation\\_constant](http://en.wikipedia.org/wiki/Acid_dissociation_constant).

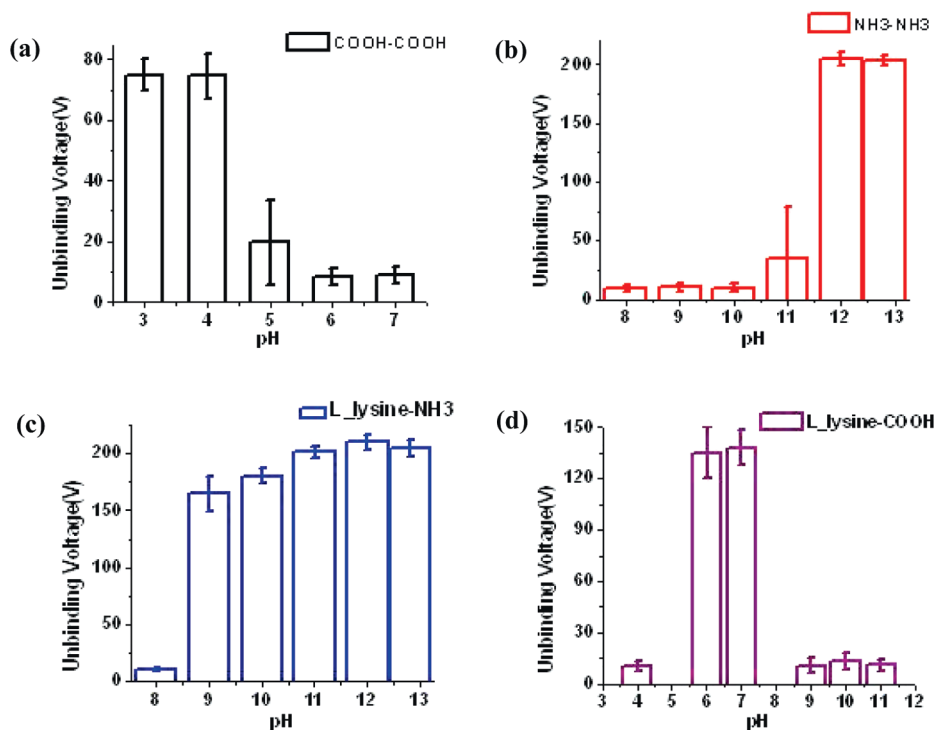


**Figure 3.** Unbinding voltage when 90% of the functionalized beads were removed from the functionalized surfaces, as function of pH: (a) carboxyl-terminated functionalized beads with 15  $\mu\text{m}$  diameter and the oxide surface functionalized by succinic anhydride presenting a carboxyl group, (b) amino-terminated functionalized beads with 10  $\mu\text{m}$  diameter and the oxide surface functionalized by APTES presenting at  $\text{NH}_3^+$  group, (c) amino-terminated functionalized beads with 10  $\mu\text{m}$  diameter and L-lysine functionalized oxide surface, and (d) carboxyl-terminated functionalized beads with 15  $\mu\text{m}$  diameter and the oxide surface functionalized by L-lysine.

**Table 1. Variation of the Unbinding Voltage as a Function of Sodium Chloride to the Medium**

	unbinding voltage (average $\pm$ standard deviation) (V)			
	DI water	0.1 mM NaCl	1 mM NaCl	10 mM NaCl
COOH-L-lysine (pH 7) <sup>a</sup>	127 $\pm$ 14	54 $\pm$ 10	19 $\pm$ 11	14 $\pm$ 2
$\text{NH}_3\text{-NH}_3$ (pH 12) <sup>b</sup>	207 $\pm$ 4	191 $\pm$ 15	11 $\pm$ 3	11 $\pm$ 3
COOH-COOH (pH 4) <sup>c</sup>	68 $\pm$ 3	varied (8–57)	not measurable	not measurable

<sup>a</sup> Carboxyl-coated beads and the L-lysine surfaces at pH 7.  
<sup>b</sup> Amino-coated beads and the APTES functionalized surface at pH 12.  
<sup>c</sup> Carboxyl-coated beads and the succinic anhydride functionalized surfaces at pH 4.

### Calculation of Dielectrophoretic Force at the Unbinding Voltage and Contact Area between the Bead and the Surface.

We correlate the unbinding voltage to the actual force of interaction by calculating the DEP force on the bead. As noted earlier, a bead located on the functionalized oxide at the center of the electrode is only affected by a vertical negative DEP force. This DEP force can be calculated by eqs 2 and 3.<sup>18</sup>

$$\vec{F}_{\text{total}} = \sum_0^{\infty} -\nabla U_n \quad (2)$$

$$U_n = -\frac{2\pi\epsilon_m K_n r^{(2n+1)}}{(2n+1)!!} \sum_{i+j+k=n} \frac{1}{i!j!k!} \left[ \frac{\partial^n \Phi}{\partial x^i \partial y^j \partial z^k} \right]^2 \quad (3)$$

where  $\Phi$  refers to electrostatic potential, and  $K_n = (n(2n+1)(\tilde{\epsilon}_p - \tilde{\epsilon}_m)) / (n\tilde{\epsilon}_p + (n+1)\tilde{\epsilon}_m)$  is the  $n^{\text{th}}$ -order Clausius-Mossotti factor. The electric field profiles above the IDT electrode structure with 40  $\mu\text{m}$  width and 10  $\mu\text{m}$  apart were generated from a finite element program (version 5.7 ANSYS Inc.) and a Matlab (R12, Mathwork) code was developed for the calculation of DEP force based on eqs 2 and 3. Figure 4 shows the first-order calculated vertical negative DEP force as a function of the horizontal position when 1  $V_{\text{peak-to-peak}}$  with 10 MHz were applied into the IDT structure. Moreover, the contact area between a bead and a functionalized surface was calculated by  $A_{\text{contact}} = 2\pi r^2 L / (r + L) \sim 2\pi r L$ ,<sup>19</sup> for  $r \gg L$ , where  $r$  is the radius of the particle and  $L$  is the length of the molecule. The molecule structure of APTES, L-lysine, or succinic anhydride consists of 3, 4, and 5 triangles, where one triangle is component of three carbon molecules and have zigzag structure.<sup>8,20</sup> In addition, the average carbon-carbon bond length and the angle of the zigzag structure are about 154 pm and 109.5°. <sup>21</sup> Hence,  $L$  for APTES, L-lysine, and succinic anhydride is about 0.75 nm, 1.1 nm, and 1.25 nm, respectively. The contact area between the beads with 10  $\mu\text{m}$  diameter and the surface functionalized by APTES or L-lysine are about  $2.36 \times 10^{-14} \text{ m}^2$  and  $3.46 \times 10^{-14} \text{ m}^2$ , respectively. The contact area between the beads with 15  $\mu\text{m}$  diameter and the surface functionalized by L-lysine or succinic anhydride are about  $5.18 \times 10^{-14} \text{ m}^2$  and  $5.89 \times 10^{-14} \text{ m}^2$ , respectively. In the first approximation, the contact area between the beads and the surface is equivalent to the half

(19) Zheng, Y.; Rundell, A. *IEEE Trans. Nanobiosci.* **2003**, *2*, 14–25.

(20) <http://commons.wikimedia.org/wiki/File:L-lysine-skeletal.png>.

(21) <http://science.csustan.edu/stone/2090/stearic.htm>.

(18) Jones, T. B.; Washizu, M. *J. Electrostat.* **1996**, *37*, 121–134.

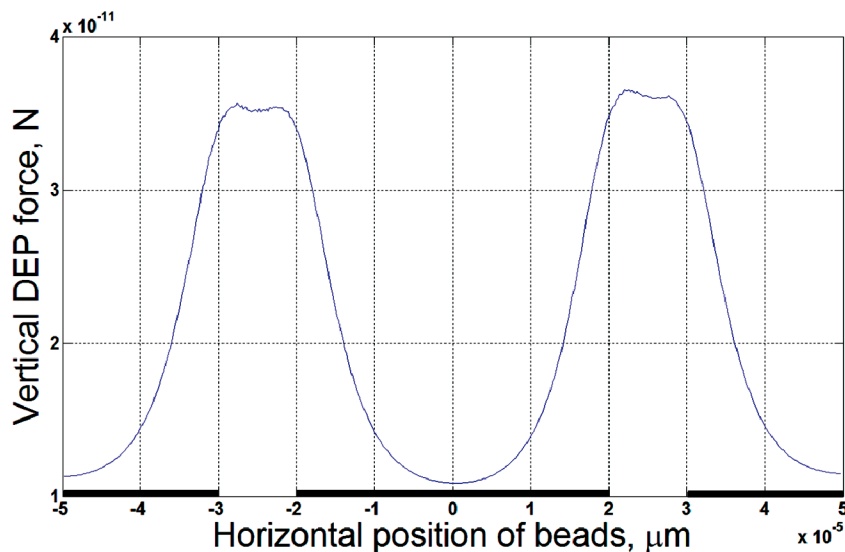


**Figure 4.** First-order calculated vertical DEP force ( $n = 1$ ) at the height of the center of the particle with  $7.5 \mu\text{m}$  radius located on the oxide surface (thickness =  $0.8 \mu\text{m}$ ) above the center of electrode when  $1 V_{\text{peak-to-peak}}$  is applied into the IDT structure.

surface area of sphere with a radius, resulting in the equation of radius of curvature

$$R = \sqrt{\frac{A_{\text{contact}}}{2\pi}} \quad (4)$$

#### Estimation and Verification of the Intermolecular Interaction Forces between Molecules on the Bead and the Surface.

Using the simulation results for the negative DEP force and the radius of curvatures, the unbinding voltage dependence on pH, and the chemical groups, the corresponding intermolecular forces can be estimated by models whose schematic diagrams are shown in Figure 5. In the region below pH 4 in Figure 5a,  $F_2$  would consist of gravity ( $4/3 \pi r^3 (\rho_p - \rho_m) g$  where  $g \sim 10^{-13} \text{ N}$ ), the van der Waals–London interaction, and the hydrogen bond, where  $r$  ( $= 5$  or  $7.5 \mu\text{m}$ ) is the radius of the particle,  $\rho_m$  ( $= 1 \times 10^3 \text{ kg/m}^3$ ) and  $\rho_p$  ( $= 1.05 \times 10^3 \text{ kg/m}^3$ ) refer to the densities of the particle and medium, and  $g$  ( $= 9.8 \text{ m/s}^2$ ) is the gravitational acceleration constant. The force to pull the bead off the surface  $F_1$  is  $7 \times 10^{-9} \text{ N}$  for the  $15 \mu\text{m}$  diameter carboxyl coated bead, which is calculated by the simulation at the unbinding voltage shown in Figure 3a, where the radius of curvature contacting the surface would be expected to be about  $90 \text{ nm}$  by eq 4. Since the dominant effect is the hydrogen bond among the components of  $F_2$ , the calculated DEP force would be equivalent to the forces of interaction of the hydrogen bond when the interaction between the neutralized carboxyl coated bead and the neutralized surface functionalized by succinic anhydride is broken at the unbinding voltage, where the acid dissociation constants ( $\text{p}K_a$ ) of carboxyl group in the succinic anhydride is  $4.2$ .<sup>14</sup> The calculated value for the hydrogen bond matches well to the force between two neutralized carboxyl-terminated groups ( $\sim 10^{-9} \text{ N}$ ) when the AFM tip with  $60 \text{ nm}$  radius was used to examine this interaction.<sup>22</sup>

In the region of force greater than  $1 \text{ nN}$  in Figure 5b, the intermolecular force  $F_2$  between the  $10 \mu\text{m}$  diameter amino-

functionalized beads and the surface functionalized by APTES or L-lysine would consist of the van der Waals–London interaction, gravity, and the hydrophobic interaction, where the radius of curvature between the bead and the surface of APTES or L-lysine is about  $61$  or  $74 \text{ nm}$  by eq 4, respectively. Among these forces, the hydrophobic interaction is dominant. In addition, the calculated vertical negative DEP force for the amino coated bead,  $F_1$ , is  $1.2 \times 10^{-8}$  to  $1.8 \times 10^{-8} \text{ N}$  between pH 9 and pH 13. Hence, the unbinding force to break the hydrophobic interaction is also about  $1.2 \times 10^{-8} \sim 1.8 \times 10^{-8} \text{ N}$ . This result is also very close to the hydrophobic interaction force between two neutralized amino-terminated groups ( $\sim 10^{-8} \text{ N}$ ) measured by the AFM tips with radius between  $30$  and  $130 \text{ nm}$ .<sup>23</sup> Moreover, the unbinding force using the APTES coated surface is clearly distinguishable from the L-lysine coated surface between pH 9 and pH 12. These phenomena can be explained by the difference between acid dissociation constants ( $\text{p}K_a$ ) of L-lysine and APTES originating from the number of amino group of both molecules, where the number of amino-terminated molecules in the tail group is one for the APTES functionalized surface and two for the L-lysine functionalized surface. Since the individual  $\text{p}K_a$  of two amino-terminated molecules in the tail of the L-lysine SAM on the oxide surface is  $8.90$  and  $10.28$ ,<sup>12</sup> their neutralization starts around pH 9 and ends around pH 11, resulting in the gradual change of unbinding force in this range of pH. On the other hand, when APTES is used for functionalizing the surface, the unbinding force is dramatically increased between pH 11 and pH 12, since the  $\text{p}K_a$  of one amino group of APTES is  $11$ .<sup>13</sup>

There is an ionic bond between pH 5 and pH 8 in Figure 3d. The van der Waals–London interaction and gravity is also added to the force  $F_2$ , attracting the carboxyl coated bead to the L-lysine functionalized surface. Since the ionic bond is dominant among the component of  $F_2$ , the calculated DEP force,  $1.7$ – $1.9 \times 10^{-8} \text{ N}$  for the bead at the unbinding voltage shown in Figure 3d would be equivalent to the force correlated to the ionic bond

(22) Noy, A.; Vezenov, D. V.; Lieber, C. M. *Annu. Rev. Mater. Sci.* **1997**, *27*, 381–421.

(23) Vezenov, D. V.; Noy, A.; Rozsnyai, L. F.; Lieber, C. M. *J. Am. Chem. Soc.* **1997**, *119*, 2006–2015.

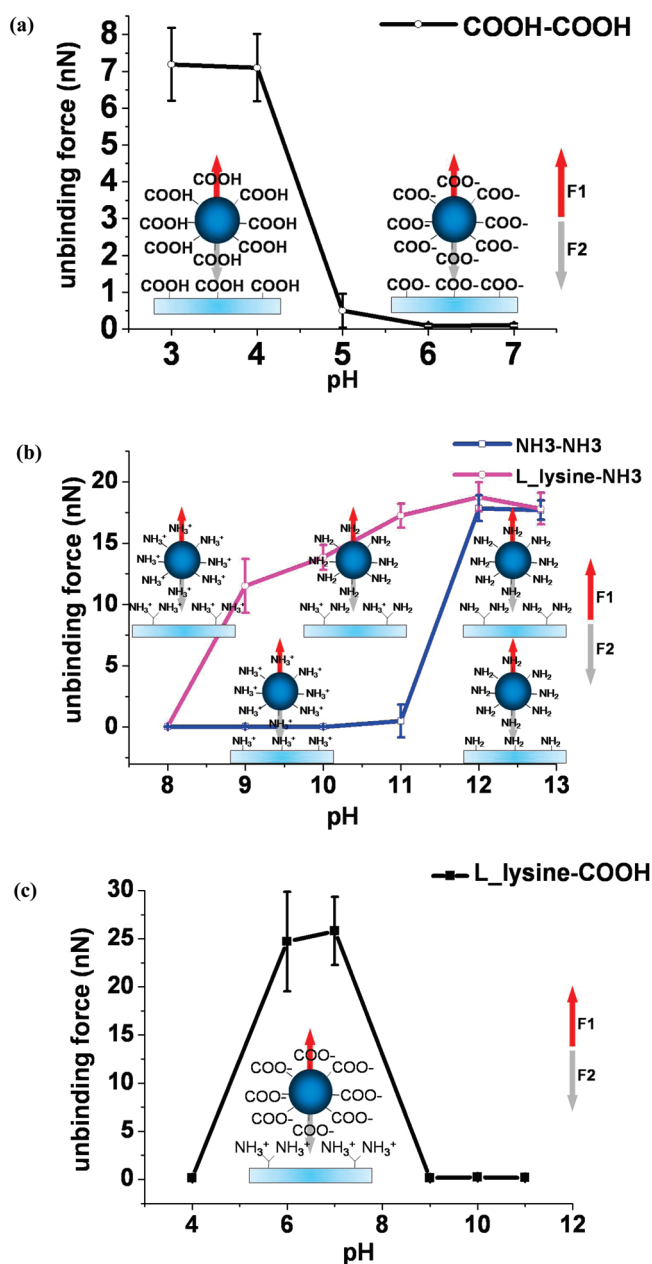


**Figure 5.** Unbinding force of functionalized beads and functionalized surface as function of pH using calculated vertical DEP force at the unbinding voltage, where (a) carboxyl-terminated functionalized beads with 15  $\mu\text{m}$  diameter and the succinic anhydride functionalized surface, (b) amino-terminated functionalized beads with 10  $\mu\text{m}$  diameter and the APTES or L-lysine functionalized surface, and (c) carboxyl-terminated functionalized beads with 15  $\mu\text{m}$  diameter and the L-lysine functionalized surface.

between pH 5 and pH 8 in Figure 5c. In the region of force much less than 1 nN in Figure 5a,b, no hydrogen bond and hydrophobic interaction exist because carboxyl-terminated molecules or amino-terminated molecules have the same charge polarity, respectively. Hence, the force  $F_2$  would be composed of gravitational forces and the van der Waals–London interaction. When the bead moved vertically from the surface at the unbinding voltage, the calculated DEP forces  $F_1$  for the amino group coated beads

and for the carboxyl group coated beads are  $4 \times 10^{-11}$  to  $6 \times 10^{-11}$  N and  $9 \times 10^{-11}$  to  $1.6 \times 10^{-10}$  N at the given unbinding voltages, respectively. These values would be equivalent to the van der Waals–London interaction since the force correlated to the van der Waals–London interaction is much greater than the gravity of the bead ( $\sim 10^{-13}$  N). Moreover, the estimated van der Waals force is in the same range ( $\sim 10^{-11}$  N) of measured van der Waals force between carboxyl-terminated molecules using AFM, where the tip radius is 20 nm.<sup>24</sup>

The minor differences between the unbinding forces shown in Figure 5 and the measured results described by the previous reports<sup>22–24</sup> would come from the differences of the estimation in the radius of curvatures between the beads and the AFM tips in contact with the surfaces. In addition, the error in surface charged density of the functional groups at the contact area between the functionalized beads and the surface is another reason. To know the precise molecular–scale interactions, more characterization of the contact area between the bead and the surface will be needed. However, our approach proves to be consistent with the experimental results reported previously with an AFM, has a high enough resolution to distinguish between the acid dissociation constant for intermolecular interactions, and is cheap and simple to implement.

## CONCLUSION

We have developed a microfluidic device based the dielectrophoretic techniques for evaluating intermolecular interactions in a simple and robust manner. Using this technique, we showed that the measured unbinding voltages can be correlated to that of intermolecular interactions originating due to differences in chemical structures and acid dissociation constants of the molecules involved. The unbinding forces to break the molecular interactions, as obtained by the measured unbinding voltage and models used to calculate the DEP forces, are consistent with the experimental results reported previously with AFM. In future studies, the surface charged density of the functional groups will be further investigated to examine the precise molecular–scale interaction. In addition, a method for automated nonoptical determination of bead detachment will help in reducing the error generated by the manual method used in this study. The technology described here would be very useful to examine intermolecular interactions using a low cost and easy to implement technique within a microfluidic device and can also be used for other applications such as measurement of mechanical properties of cells and biomolecules.

## ACKNOWLEDGMENT

This work was supported by the Korea Research Foundation (KRF-2007-313-D00963 and KRF-2008-313-D00580) and the KOSEF (R01-2008-000-11338-0).

Received for review June 3, 2009. Accepted July 17, 2009.

AC901211B

(24) Jean, M. S.; Hudlet, S.; Guthmann, C.; Berger, J. J. *Appl. Phys.* **1999**, *86*, 5245–5248.